Thermodynamics and dielectrics of polymerization, crystallization and interfacial phenomena

1999 J. Phys.: Condens. Matter 11 A317

(http://iopscience.iop.org/0953-8984/11/10A/029)

J. Phys.: Condens. Matter **11** (1999) A317–A327. Printed in the UK PII: S0953-8984(99)01060-7

Thermodynamics and dielectrics of polymerization, crystallization and interfacial phenomena

E Tombari†, C Ferrari†, G Salvetti† and G P Johari‡

† Istituto Fisica Atomica e Molecolare del CNR, via del Giardino 7, 56127-Pisa, Italy
‡ Department of Materials Science and Engineering, McMaster University, Hamilton, Ontario, Canada L8S 4L7

Received 2 October 1998

Abstract. Several types of dielectric and calorimetric measurements have been made simultaneously on chemically and physically changing systems, e.g., systems undergoing polymerization and crystallization, in real time using newly developed equipment. The relaxation times, τ_0, obtained at a certain degree of polymerization in the temperature modulation mode and the isothermal mode are the same, although the polymerization is slower in the former case. τ_0 and direct-current conductivity do not follow the same formalism, although both change upon polymerization as if the liquid was being cooled. The heat capacity decreases on polymerization and the original GHz-frequency dielectric relaxation becomes gradually extinct. The dynamics upon heating a partially polymerized sample is not determined by further polymerization. Calorimetry and dielectric data show that the diffusion control's onset occurs gradually and not at a particular value of τ_0. The crystallization and melting of poly(ethylene glycol) of molecular weight 3400 show substantial effects arising from interfacial polarization. Its equilibrium permittivity does not follow the law of mixtures, indicating substantial contributions from changes in the dipole moment at the solid/liquid interface.

1. Introduction

Experiments that may yield relations between the molecular dynamics and chemical kinetics during polymerization are of much interest, for two reasons: (i) technological—because a procedure for monitoring the polymerization process may be developed [1–3]; and (ii) fundamental—because polymerization causes mutual slowing of both the molecular dynamics and the reaction kinetics, until both the dynamics and the reaction come to a virtual halt and the liquid is said to be vitrified. Despite this interest over nearly 60 years, it has only now become possible to study the two phenomena for one sample, simultaneously in real time. These studies have given us insights into:

(a) the polymerization kinetics;
(b) the evolution of faster relaxation processes;
(c) the occurrence of various types of reaction;
(d) the change in the heat capacity, C_p, and relations between the configurational entropy, S_{conf}, and the slowing of the molecular dynamics;
(e) the relation between the relaxation time, τ, and the extent of polymerization, α, as the reaction becomes diffusion controlled;

0953-8984/99/SA0317+11$19.50

(f) the differences among the dynamic behaviours of the polymers formed by varying the temperature–time history of the polymerization, which are related to the polymer's structure and manner of covalent bonding;
(g) the loss of chemical and physical metastabilities of a vitrified polymer;
(h) the crystallization and melting kinetics; and
(i) the interfacial effects on the formation of different phases.

These insights are useful for understanding the physics of non-equilibrium systems approaching spontaneously a chemical and/or physical equilibrium at an almost imperceptible rate, and for identifying the various stages in a commercial process, such as in the production of polymer composites, adhesives, microelectronics and data-storage devices. It is also of fundamental importance in revealing the negative feedback between molecular diffusion and chemical reaction that vitrifies a liquid ultimately. Here we describe briefly some of these experiments and the insights gained.

2. Experimental methods

An instrument, Simultaneous Impedance and Thermal Analyser (SITA), was developed specifically for carrying out studies in real time of thermodynamics and dielectric spectroscopy (45 Hz–0.5 MHz) during chemical and physical change. Briefly, it consists of a pair of concentric electrodes which act as a dielectric cell of 14 pF nominal capacitance. This cell is contained in a calorimeter. Calorimetry and dielectric spectroscopy are thus performed on one sample in pre-programmed temperature–time, T–t, modes, both isothermally and during controlled heating and cooling. The details of this instrument and its operation, and the accuracy of the data obtained, have been described before [4]. As these studies advanced, a variable-amplitude and variable-frequency sinusoidal temperature modulation mode was incorporated into SITA. This allows one to determine the real and imaginary components of C_p along with the dielectric spectra, an improvement over the earlier method [5].

Diglycidyl ether of butanediol (DGEBD), the amines and poly(ethylene glycol) of molecular weight 3400 (PEG-3400), were purchased from Aldrich Chemicals, and used as received. The source and properties of the diglycidyl ether of bisphenol-A (DGEBA) have been given before [6]. All mixtures were prepared accurately by weight, and mechanically mixed for 1 min. The physical changes with t and T do not need description, as the addition reactions in the DGEBA–diamine mixture that vitrify the initial liquid mixture, when the temperature of curing is lower than the glass transition temperature of the fully reacted mixture [7, 8].

3. Results and discussion

3.1. Thermodynamics and molecular dynamics during polymerization

A typical T–t profile for the polymerization of a stoichiometric ethylene diamine–DGEBA mixture for the normal and modulated modes of SITA at 298.2 K is shown in figure 1(A). The rate of the enthalpy release, $(\mathrm{d}H/\mathrm{d}t)_T$, is shown against t in figure 1(B) for both modulated cases. The rate $(\mathrm{d}H/\mathrm{d}t)_q$, q being the heating rate, in all of the T-ramp parts of the T–t profile (figure 1(A)) was determined and is shown in figure 1(C). The area under the $(\mathrm{d}H/\mathrm{d}t)_q$–$T$ plot divided by q plus the area under all of the $(\mathrm{d}H/\mathrm{d}t)_T$-against-$t$ plot is equal to the heat of polymerization, ΔH^0, which was 230.5 ± 1.5 kJ mol^{-1} for DGEBA. The extent of reaction, α, is equal to $[\Delta H(t)/\Delta H^0]_t$. Assuming that the energy per covalent bond formed is independent

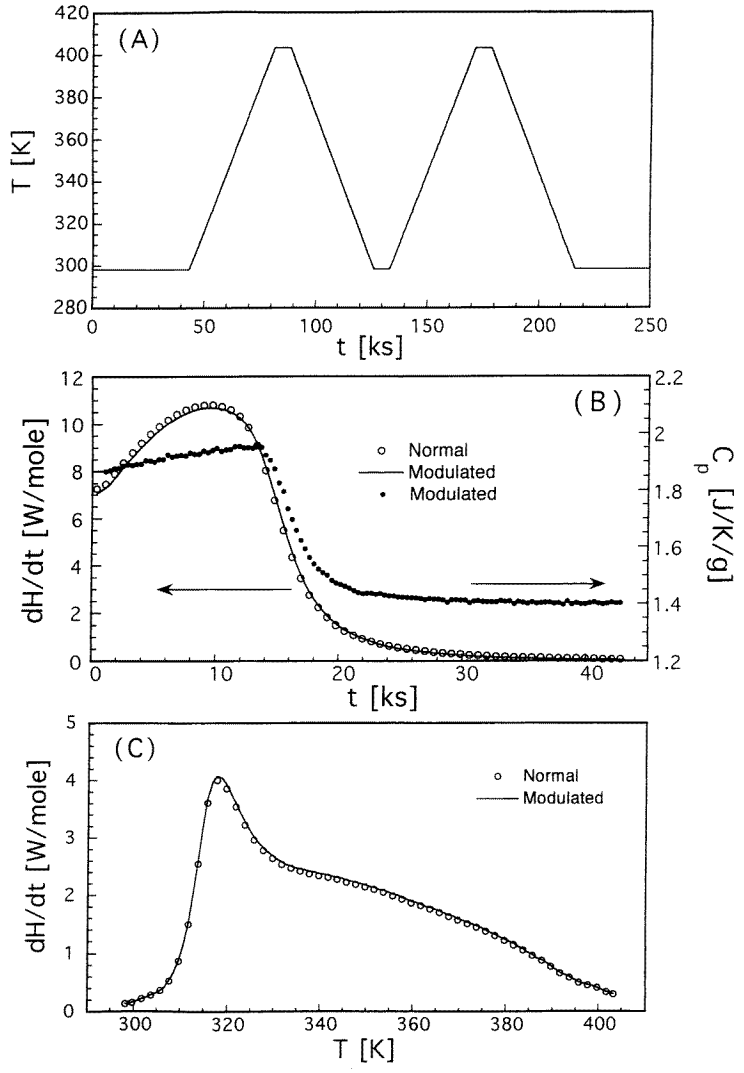

Figure 1. (A) The T–t profile for calorimetry and dielectric measurements of ethylene diamine–DGEBA mixture in normal and modulated modes. (B) The rate at which heat evolved during polymerization at 298.2 K (the scale on the left) and C_p at 2.7 mHz (the scale on the right). (C) The rate at which heat evolved during the ramp-heating measurements.

of the number of existing bonds and the structure of the liquid, the number of bonds formed is

$$n = \zeta N_A \alpha$$

where ζ is the number of covalent bonds formed by stoichiometric molecular amounts of DGEBA with the amines [8] and N_A is the Avogadro number. Both α and n are plotted against t in figure 2(A). Thus the dielectric data in the t-regime can be converted to data in the α- or in n-regime. The difference between the α obtained from the normal and modulated experiments is expected to be significant, but is not clearly evident in figure 2(A). Nevertheless, the dc conductivities, σ_0, at a given t differed in the two experiments, as did the relaxation times, τ_0. This difference vanished when plots were constructed against α instead of t.

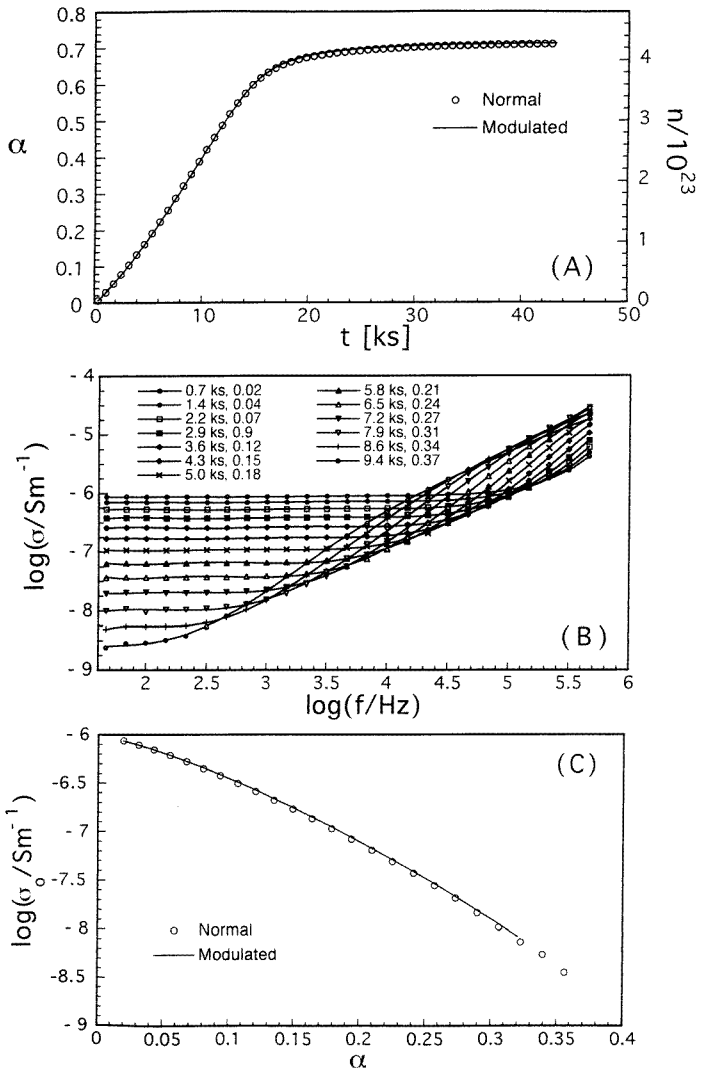

Figure 2. (A) The extent of reaction is plotted against the polymerization time of ethylene diamine–DGEBA mixture at 298.2 K for the two modes. (B) The conductivity spectra at different t and α at 298.2 K for the normal mode. The full curves are interpolations between experimental points included to assist in the reading of the spectra. (C) σ_0 is plotted against α for the normal and modulated modes.

As an example, typical conductivity (σ-) spectra are shown in figure 2(B), from which the dc conductivity, σ_0, was determined as a function of α. The plot of this is shown in figure 2(C). The spectra of the dielectric permittivity and loss, ε' and ε'', are shown in figures 3(A) and 3(B). The ε'-spectra show small contributions from interfacial polarization at low values of α when σ_0 is relatively large. These decrease as σ_0 decreases. The spectra were analysed in terms of stretched-exponential relaxation, which gave the characteristic relaxation time, τ_0, the stretch parameter, β, and the equilibrium permittivity, ε_s. For direct comparison against σ_0, $(\tau_0)^{-1}$ is plotted in figure 4(A). This clearly demonstrates that σ_0 and $(\tau_0)^{-1}$ are not linearly related, contrary to the usual assumption. β was found to be 0.36, constant with increasing α

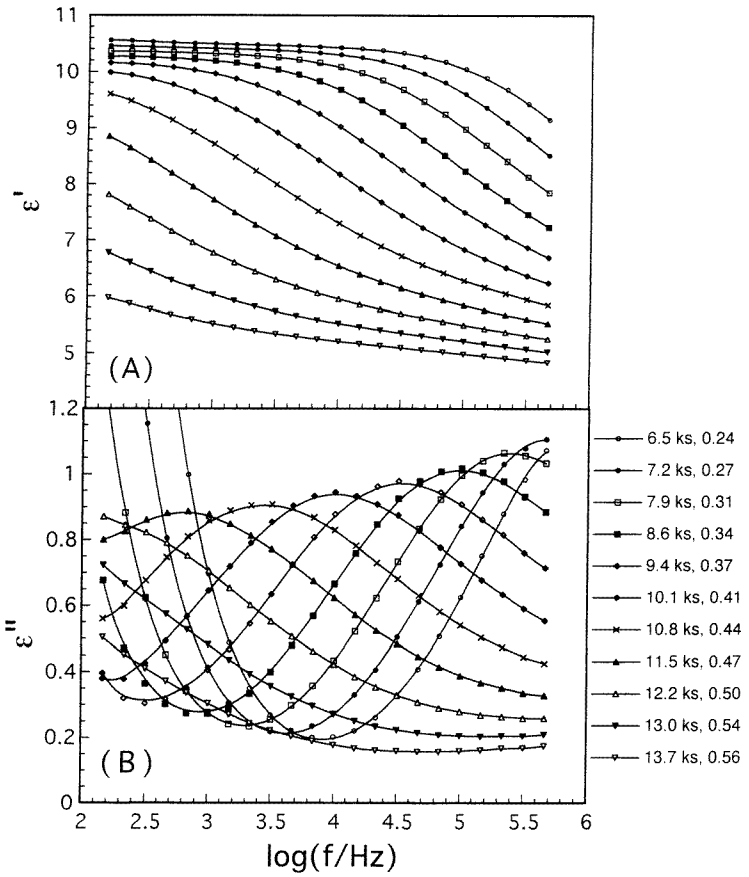

Figure 3. The ε'- and ε''-spectra at different α during polymerization of an ethylene diamine–DGEBA mixture in the kHz frequency range at 298.2 K. The full curves are interpolations between experimental data.

in the range where τ_0 was determined, and ε_s is plotted against α in figure 4(B). The decrease in $(\tau_0)^{-1}$ with increase in α is described by the empirical equation [9]

$$[\tau_0(n)]^{-1} = [\tau_0(n=0)]^{-1} \exp[-(S\alpha^p)] \tag{1a}$$

where

$$S = \ln[\tau_0(\alpha = 1)/\tau_0(\alpha = 0)]$$

is a T-dependent parameter, which is experimentally determined and p is an empirical parameter that describes the rate of approach to vitrification. Equation (1a) is combined with the Adam–Gibbs equation [10] for S_{conf} to obtain

$$S_{conf} = C/[T\Omega + TS(\alpha)^p] \tag{1b}$$

where C is a constant as defined in reference [10], and

$$\Omega = \ln[\tau(\alpha = 0, T)/\tau(\alpha, T \to \infty)].$$

Thus S_{conf} becomes related to α, but only in relative terms. Nevertheless, such correlations have been useful in the understanding of the structural aspects of molecular dynamics [11–13].

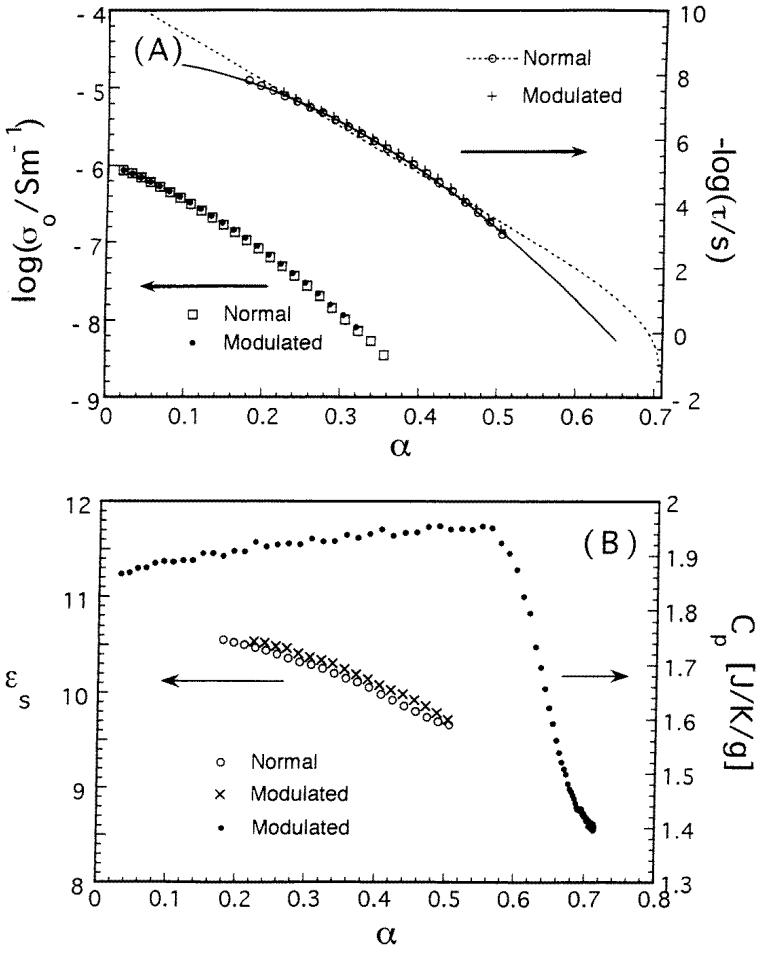

Figure 4. (A) Logarithmic plots of σ_0 and $(\tau_0)^{-1}$ against α for the two modes. The continuous curve was calculated from equation (1) and the dashed curve from equation (3). (B) ε_s and C_p measured at 2.77 mHz are plotted against α.

Further studies [14] of the original spectra in the GHz frequency range of polymerization in separate but complementary experiments, as shown in figure 5, have shown that this original relaxation dynamics remains unaffected by the decreasing S_{conf} of the liquid, i.e., that the dynamics of the new relaxation process, which evolves as n increases, is determined by S_{conf} for the liquid and that the dynamics of the original one in the GHz range is not, only its strength decreases with S_{conf}, or n.

When the partially polymerized sample is heated at 10 K h^{-1} (ramp 1 in figure 1(A)), the increase in thermal energy should (a) decrease τ_0 for the primary relaxation process, (b) increase the characteristic frequencies of the secondary relaxation processes, and (c) increase τ_0 because further polymerization occurs, as is evident from figure 1(C). Thus the ε'- and ε''-spectra at different t, T and α in figure 6 are useful for determining the process that predominates. The spectra show that the peak, which had moved to lower frequencies during isothermal polymerization, could not be brought back into the spectral window. The effects (a) and (b) outweigh effect (c).

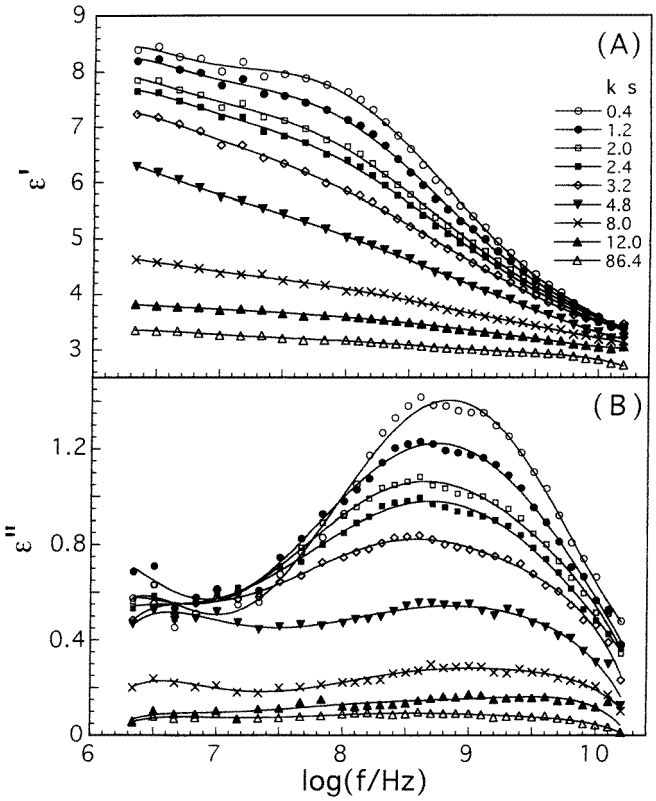

Figure 5. The ε'- and ε''-spectra of a 5 mol% dimethylbenzylamine–DGEBA mixture in the GHz frequency range at different times of polymerization at 335.4 K. The full curves are interpolations between experimental data points.

3.2. Polymerization kinetics, molecular dynamics and diffusion control

Before vitrification, a liquid's polymerization becomes diffusion controlled, but the diffusion control's onset is expected to be gradual, not abrupt at a certain t, α or n. Nevertheless, it has been concluded that this onset can be determined from the profile of the plots of $(\mathrm{d}\alpha/\mathrm{d}t)/(1-\alpha)$ against α, and that the values of t and α at which the ε''-peak appears, at 1 Hz or less, is a 'quantitative indicator' for the diffusion control's onset [15]. Briefly, the profile of such plots is given by an empirical relation:

$$\mathrm{d}\alpha/\mathrm{d}t = (k_1 + k_2\alpha)(1-\alpha)^2\left[\frac{2}{1+\exp[(\alpha-\alpha_f)/b]} - 1\right] \tag{2}$$

where the notation is the same as in reference [15], the normalization factor being dropped.

Accordingly, $(\mathrm{d}\alpha/\mathrm{d}t)/(1-\alpha)$ initially increases slowly, reaches a maximum and then decreases rapidly after α has reached α_f. The rapid decrease is seen as an indicator of the diffusion-control onset [15].

The use of SITA in the normal mode has made possible an examination of this conclusion's merits. We studied polymerization to (i) a network polymer (from an EDA–DGEBA mixture) which vitrified isothermally and (ii) a network polymer (from an HMDA–DGEBD mixture) which did not vitrify and whose dielectric relaxation time remained below a few μs after complete reaction ($\alpha = 1$). The latter study was necessary to ascertain whether a relaxation

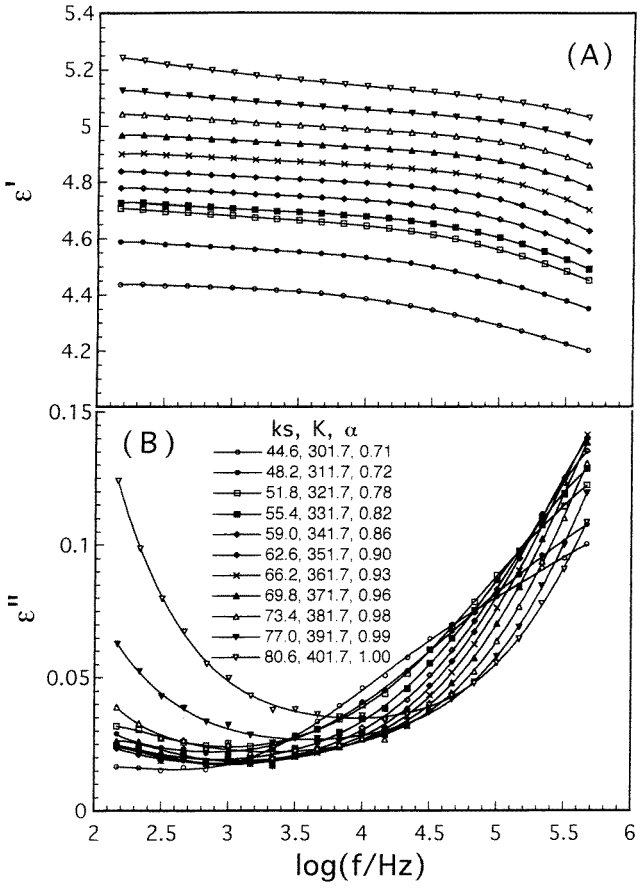

Figure 6. The ε'- and ε''-spectra at different t, T and α during the polymerization of an EDA–DGEBA mixture during ramp heating at 10 K h^{-1} after partial polymerization. The full curves are interpolations between experimental data points.

rate can be unambiguously associated with the onset of a rapid decrease in the plots of $(\mathrm{d}\alpha/\mathrm{d}t)/(1-\alpha)$ against α. The results are shown in figures 7(A) and 7(B), where the best continuous curve calculated from equation (2) is also shown. Evidently, the sharp bending of the plots of $(\mathrm{d}\alpha/\mathrm{d}t)/(1-\alpha)$ against α also occurs near a certain value of α for the second study at high values of α (α_f for this composition is 1). But even when $f_m > 10^5$ Hz in this case on complete polymerization ($\alpha = 1$) and the liquid remains soft and easily deformable after the complete reaction [7], the sharp bending of the plot of $(\mathrm{d}\alpha/\mathrm{d}t)/(1-\alpha)$ against α still occurs. This is evidence that such sharp bending is not an indication of the onset of diffusion control during polymerization at $f_m \sim 1$ Hz. Equation (2) also deviates from the data far too much, even qualitatively, to be reliable. We conclude that diffusion control does not begin at $f_m = 1$ Hz, or near it.

The relaxation rate, f_m, has also been related to α by [15]

$$\log(f_m(\alpha)) = a(T)\left[\log(f'_m(0) - \frac{k_p\alpha}{\ln(10)}\right] + \log\left[\frac{2}{1+\exp[(\alpha-\alpha_f(T))/b]} - 1\right] + c(T) \tag{3}$$

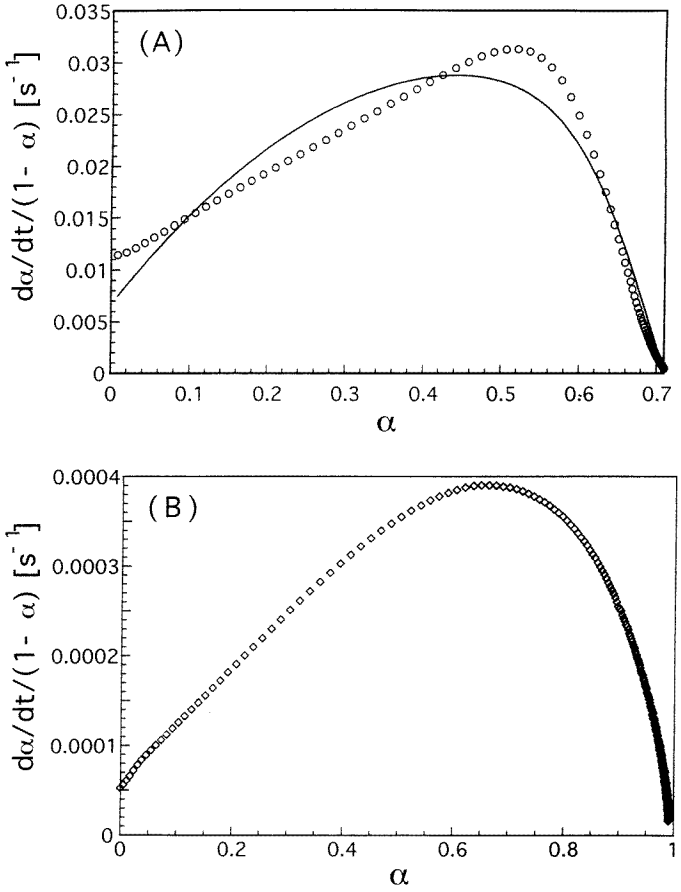

Figure 7. (A) $(\mathrm{d}\alpha/\mathrm{d}t)/(1-\alpha)$ for a stoichiometric EDA–DGEBA mixture is plotted against the extent of reaction during the course of polymerization at 298.2 K. The continuous curve is the best fit from equation (2). (B) The corresponding plot for a stoichiometric HMDA–DGEBD mixture at 323.2 K, which polymerizes completely to a gel-like structure without vitrifying at $\alpha = 1$.

with the notation being the same as in reference [15]. Accordingly, $\log(f_m(\alpha))$ decreases linearly as α increases from its zero value until the diffusion control has its onset, and then bends sharply downwards when $\alpha \to \alpha_f$. The best fit of equation (3) to the data is shown by the dashed curve in figure 4(A). Clearly, the shape of the best-fit plot is very different from that for the measured values. We conclude that diffusion control does not begin at $f_m = 1$ Hz, or near it.

3.3. Thermodynamics and dielectrics during crystallization

Figures 8(A)–8(C) show the plots of α_{crys} and of ε' at 0.5 MHz for PEG-3400 against T, and the deduced plots of ε' against α_{crys}, for the heating and cooling, both at 10 K h^{-1}, during which the sample melted and crystallized. The data obtained for the normal and modulated modes seem to agree within the experimental errors. The hystereses in the plots in figures 8(A) and 8(B) largely vanish, when the ε'- and α_{crys}-data are used at the reference temperature of 330 K, as shown in figure 8(C). Because there is no dipolar relaxation in this frequency range

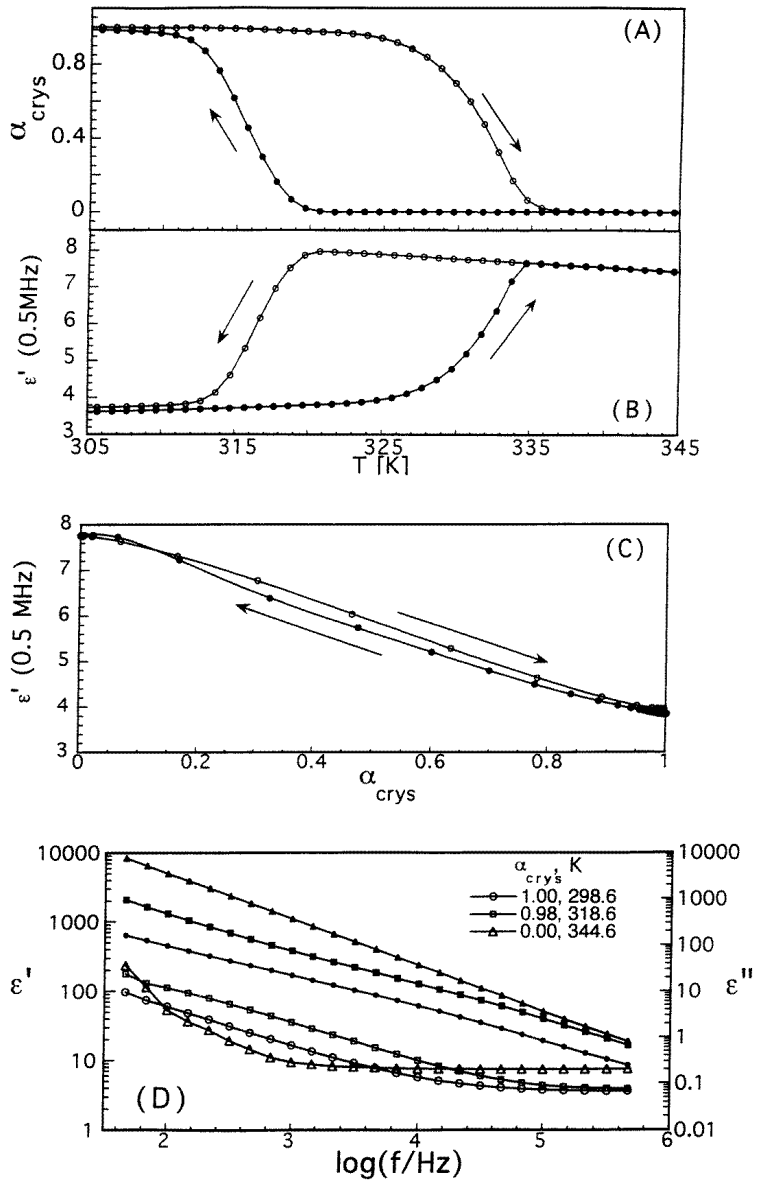

Figure 8. (A) The plots of α_{crys} against T. (B) The plots of ε' at 0.5 MHz against T. (C) The plots of ε' at 0.5 MHz against α_{crys} determined from the plots in (A) and (B) after extrapolating to ε' at 330 K. (D) The ε'-spectra (open symbols) and ε''-spectra (filled symbols) of PEG-3400 at three values of α_{crys} and T during the heating and cooling at 10 K h^{-1}. Note that α may not reach unity, because of the presence of amorphous phase at crystal junctions in a polycrystalline polymer. The full curves are in every panel interpolations of experimental data points.

in the low-viscosity ($\sim$1 P) molten PEG-3400, ε' at 0.5 MHz corresponds to ε_s. The difference between the ε_s for the same α_{crys} and the non-linearity of the plots indicates that the law of mixtures is not obeyed. It seems that dipolar interactions at the solid–liquid interface alter the net ε_s of the mixtures.

3.4. Interfacial effects in semicrystalline samples

An example of this effect is seen in figure 8(D), where the ε'- and ε''-spectra of PEG-3400 at three values of T and three values of α_{crys} show very large values at low frequencies. Evidently, the interfacial polarization arising from the Maxwell–Wagner effect is substantial at high values of α_{crys}. These effects of α_{crys} on the dielectric behaviour will be described further elsewhere.

4. Conclusions

The use of SITA has allowed us to investigate relations between the thermodynamics and molecular or physical and chemical kinetics of a variety of processes. The complete study has so far been only of the polymerization process. Detailed investigations of other processes are yet to be made.

Acknowledgments

GPJ is grateful for the hospitality of the IFAM group and support from CNR, Italy.

References

[1] Barton J M 1985 *Adv. Polym. Sci.* **72** 111
[2] Senturia S and Sheppard S 1986 *Adv. Polym. Sci.* **80** 1
[3] Johari G P 1993 *Chemistry and Technology of Epoxy Resins* ed B Ellis (London: Chapman and Hall) p 175 and references therein
Richert R and Blumen A (ed) 1994 *Disorder Effects on Relaxational Processes* (Berlin: Springer) p 627
[4] Tombari E, Ferrari C, Salvetti G and Johari G P 1996 *Nuovo Cimento* D **18** 1443
[5] Ferrari C, Salvetti G, Tombari E and Johari G P 1996 *Phys. Rev.* E **54** R1058
[6] Tombari E, Ferrari C, Salvetti G and Johari G P 1998 *J. Polym. Sci., Polym. Phys.* **36** 303
[7] Cassettari M, Salvetti G, Tombari E, Veronesi S and Johari G P 1992 *Nuovo Cimento* D **14** 763
[8] Ferrari C, Tombari E, Salvetti G and Johari G P 1998 *J. Chem. Soc. Faraday Trans.* **94** 1293
[9] Tombari E and Johari G P 1992 *J. Chem. Phys.* **97** 6677
[10] Adam G and Gibbs J H 1965 *J. Chem. Phys.* **43** 139
[11] Tombari E, Ferrari C, Salvetti G and Johari G P 1998 *J. Phys.: Condens. Matter* **9** 7017
[12] Johari G P, Wasylyshyn D A and McAnanama J A 1996 *J. Chem. Phys.* **105** 10 621
[13] Wasylyshyn D A, McAnanama J A and Johari G P 1998 *J. Chem. Soc. Faraday Trans.* **91** 343
[14] Wasylyshyn D A, Johari G P, Tombari E and Salvetti G 1997 *Chem. Phys.* **223** 313
Wasylyshyn D A, Johari G P, Tombari E and Salvetti G 1997 *J. Phys.: Condens. Matter* **9** 10 521
[15] Fournier J, Williams G, Duch C and Aldridge G A 1996 *Macromolecules* **29** 7097